International Journal of Pharmaceutics, 53 (1989) 13–24
Elsevier

IJP 01780

Visualisation of normal and enhanced $HgCl_2$ transport through human skin in vitro

H.E. Boddé [1], M.A.M. Kruithof [1], J. Brussee [2] and H.K. Koerten [3]

[1] *Center for Bio-Pharmaceutical Sciences, Leiden (The Netherlands),* [2] *Department of Organic Chemistry, Gorlaeus Laboratories, Leiden (The Netherlands) and* [3] *Department of Electron Microscopy, State University of Leiden, Leiden (The Netherlands)*

(Received 20 July 1988)
(Modified version received 12 October 1988)
(Accepted 15 December 1988)

Key words: Visualization; In situ precipitation; Human skin; Mercuric Chloride; Penetration enhancer; Azone; Dimethylsulfoxide; Propylene glycol; Transmission electron microscopy

Summary

The aim of the present study was to visualize the routes of penetration of mercuric chloride through human skin in vitro at the ultrastructural level, and to clarify the influence of some penetration enhancers (dimethylsulfoxide (DMSO), propylene glycol and hexyl, dodecyl and hexadecyl azone) PBS-pretreated skin (used as a control) or enhancer-pretreated skin was subjected to an in vitro mercuric chloride diffusion experiment in a bicompartmental polycarbonate diffusion cell Upon interrupting the diffusion experiment, skin samples were treated with ammonium sulphide vapour to precipitate the mercury in the form of mercuric sulphide, then processed for Transmission electron microscopy The presence of mercury in the precipitates was verified using X-ray microanalysis The results indicate, that the intercellular route of transport through the stratum corneum predominates, but that after longer transport times, apical corneocytes tend to take up some material, leading to a typical bimodal distribution of mercury, predominantly *inside* apical corneocytes, predominantly *between* medial and proximal corneocytes There were no signs for a discontinuity in the in depth distribution of mercury in that an almost unmountable barrier would exist in the lower region of the stratum corneum, as suggested by e g Sharata and Burnette (1987, 1988), however, there was evidence for the presence of two types of cells, apical corneocytes, which tend to take up mercuric ions relatively easily, and medial and proximal corneocytes, which are less capable of doing so Hexyl azone and DMSO "enhanced" but did not qualitatively change the "bimodal" in depth distribution of mercury Finally, dodecyl azone proved to be an effective enhancer and furthermore favoured intercellular transport of the mercury at the expense of cellular uptake

Introduction

One of the bottlenecks for a successful development of transdermal drug delivery devices is the fact, that the skin (more accurately, the stratum corneum) tends to control the rate of drug transport. This makes it very difficult to influence or regulate the transdermal drug absorption kinetics from outside, i.e. by the vehicle. A possible and even elegant solution may be the use of so called "penetration enhancers" in order to suppress the dominating role of the stratum corneum penetration barrier. Ideally, one should possess a range of enhancers, each with its own mode of action and

Correspondence H E Boddé, Center for Biopharmaceutical Sciences, Leiden (The Netherlands)

0378-5173/89/$03 50 © 1989 Elsevier Science Publishers B V (Biomedical Division)

effectiveness, from which one could make a proper choice to be used in combination with any given drug. Although some knowledge as to the modes of action of penetration enhancers has already been acquired (Golden et al., 1986; Barry, 1987a and b; Beastall et al., 1988), the present knowledge is still fragmentary and does not yet provide a solid basis for selecting or even developing penetration enhancers for optimising specific dermal or transdermal preparations.

An aspect which needs special attention is the *route* of skin penetration, i.e. the actual pathway which the drug follows on its way through the stratum corneum and viable epidermis. One of the most direct ways of studying the route of skin penetration would be a microscopic technique with which skin structures can be visualized, and, given the proper marker, the diffusable compound (the drug) can be visualized and localized inside that structure. Various attempts have been made to do so, using light microscopy in combination with autoradiography (Fukuyama, 1985), metachromatic staining (Elling, 1986; Heine, 1983), and fluorimetry (Lopp et al., 1986). Furthermore, electron microprobe analysis has been used to visualize transepithelial sodium transport (Rick et al., 1986) at the ultrastructural level. The skin penetration of nickel and chromate ions has been studied by Malmqvist et al. (1987) using proton-induced X-ray emission (PIXE). They determined transepidermal gradients of Ni^{2+} and Cr^{2+} with about 30 μm intervals between measurements.

A simple technique used by some authors to visualize transport of diffusable compounds through skin is the so called "in situ precipitation" (Silberberg, 1968; Nemanic and Elias, 1980; Sharata and Burnette, 1987 and 1988). The latter study was based on *mouse skin*; one of its major conclusions was that for the markers used (mercuric and nickel salts) on unpretreated skin, the intercellular pathway of diffusion predominated, whereas a pretreatment with DMSO resulted in uptake of the markers by (presumably disrupted) corneocytes. A very peculiar result these authors described, was the fact that, even upon prolonged diffusion, their markers "stopped" at a certain borderline in the lower region of the stratum corneum, spread laterally, and did not move further downwards. They implied from this observation that the barrier inside the stratum corneum might be localized in its lower (proximal) region. It should, however, be borne in mind that their studies were based on mouse skin, which differs considerably from its human counterpart.

The present study aimed at visualizing routes of penetration through freshly excised human skin, using mercuric chloride as a marker and applying transmission electron microscopy. A further aim was the elucidation of the modes of action of some penetration enhancers, including azone and some newly synthesized derivatives thereof.

Materials and Methods

Skin

Fresh human mamma skin, obtained from mamma operations, was kept overnight on a moist gauze at 4 °C. On the second day, the skin was dermatomed to 110 ± 20 μm, using an Electrodermatome (Padgett). The dermatomed skin samples were cut in circular pieces (18 mm in diameter) and used for diffusion experiments on the same day.

Synthesis and characterisation of azones (N-alkyl-azacycloheptan-2-one)

General procedure for the preparation of azones: 11 g of 55–60% NaH dispersion in mineral oil (0.25 mol) were washed two times with 75 ml petroleum ether 40–60. The petroleum ether was decanted and the NaH was suspended in 250 ml dry toluene and placed in a 1 liter threeneck round bottom flask provided with a mechanical stirrer and a N_2-gas inlet. 20 g Azacycloheptan-2-one (0.177 mol) dissolved in 200 ml dry toluene was added dropwise under stirring in a dry N_2-atmosphere. After the addition the reaction mixture was refluxed during 1 h and then cooled to room temperature. Alkyl bromide (0.200 mol) mixed with 200 ml dry toluene was added dropwise. The reaction mixture was stirred under nitrogen for 24 h at room temperature followed by heating to reflux for a number of h (see Table 1) depending which alkyl bromide was used. Upon cooling the formed NaBr was filtered off and the

filtrate was concentrated by distillation under reduced pressure. The remaining oil was purified by fractional distillation under reduced pressure. The purity of the compounds was verified by NMR spectroscopy. The yield of product was 50–80%.

Pretreatments

In some cases, before starting a diffusion experiment, the skin was pretreated with one of the two following compounds: dimethyl sulphoxide (DMSO), propylene glycol (PG), 1-hexyl-aza-cycloheptane-2-one (hexyl-azone), 1-dodecyl-aza-cycloheptane-2-one (dodecyl azone), 1-hexadecylaza-cycloheptane-2-one (hexadecyl azone).

DMSO and PG were used neat, the azones were applied in a 10% v/v solution in PG. 24 h before starting a diffusion experiment, the skin samples were placed on Petri dishes (stratum corneum side up, dermis side down) and the enhancer (-solution) was poured on top of the skin (about 200 $\mu l/cm^2$) and left without occlusion; the treated skin samples were then allowed to stand for 24 h at 4°C (except in the case of DMSO, where the samples were kept at room temperature to prevent crystal formation).

PBS-treated samples were used as controls.

Diffusion experiments

The pretreated skin samples were clamped inside a two-compartment diffusion cell (made of polycarbonate), using dialysis membranes (cut-off at 5000 D) on both sides of the skin for support. The donor chamber (facing the stratum corneum) was filled with 1.5 ml of a 5% w/v solution of mercuric chloride ($HgCl_2$) in PBS, pH 7.4. The acceptor chamber contained PBS, pH 7.4. Both chambers were closed. The diffusion experiments were carried out at 33°C. After 1/4, 3/4, 1, 2, 10 and 48 h the skin samples were rinsed with PBS for 15 s, wiped dry with a tissue and divided in 3-mm-diameter samples for electron microscopy. In some cases skin samples were completely immersed in a donor solution (containing 5% $HgCl_2$ in PBS at pH 7.4) and analysed after 1/2 and 1 h. Furthermore, a number of 10 h diffusion experiments were done with the dermis facing the donor chamber, in order to study the influence of the direction of transport.

Electron microscopy

All samples were exposed to the vapour of a 25% ammonium sulphide solution to provoke the precipitation of mercuric sulphide (HgS) and thus obtain fixation and visualization of the mercury, rinsed two times 5 min in a 0.1 M cacodylate buffer (pH 7.4) at 4°C and fixed for 7 hours in a 1,5% glutaraldehyde solution in 0, 1 M cacodylate buffer (pH 7.4) at 4°C. Upon a two times five minutes rinse with cacodylate buffer, the tissue was fixed for about 10 h in a 1.0% osmiumtetroxide/2.1% potassium hexacyano ferrate (II)-solution in 0.1 M cacodylate buffer at 4°C. Upon two further 5 min rinses with 0.1 M cacodylate buffer, dehydration was carried out using an alcohol gradient of 30–50–70–80–90–100% (two times 5 min for each step up to 90%; two times 15 min for the 100%). Subsequently the tissue was impregnated for 30 min with propylene oxide at room temperature, then impregnated with a 50/50 propylene oxide/Epon 812 (DDSA : MNA ratio of 3 : 7.5) using DMP-30 as a hardener for 30 min and finally impregnated with pure Epon 812 (DDSA : MNA ratio of 3 : 7.5) for 3.5 h. Care was taken to orientate the skin samples flat and horizontally in the embedding material. Upon 4 days of hardening at 60°C the samples were cut on a LKB microtome using a diamond knife (Diatome); 70 nm (yellow–gray) sections were collected on collodion-coated copper grids (100 mesh), whereupon they were examined in a Philips EM 201 Electron Microscope operated at 80 kV. Additional staining agents were not used.

Validation of the in situ precipitation method

In order to verify the quality of fixation with the in situ precipitation method, a number of control experiments were carried out. Firstly, PBS treated specimens were subjected to a diffusion experiment (40 h), then washed for 20 h with PBS, then treated with ammonium sulphide etc. ("washed *before* precipitation"). A second series of PBS-treated specimens received a PBS wash *after* completing the ammonium sulphide treatment ("washed *after* precipitation"). In order to verify the accuracy of localization obtained with the method, some specimens were deliberately overexposed to the electron beam in the electron

microscope, so as to allow sublimation of the mercuric sulphide to find out whether the precipitates were on top of, or inside the section. Furthermore, the presence of mercury in the precipitates was verified by the use of X-ray microanalytical spot analysis. Measurements were performed with a Tracor TN 2000 energy dispersive X-ray microanalyzer attached to a Philips EM 400 electron microscope. The specimens were placed in a low background berilium holder at an angle of 18° relative to the electron beam. Measurements were done during 200 s lifetime with a spot size of 100 nm and an accelerating voltage of 80 kV.

Results

The X-ray emission spectrum given in Fig. 1 was taken at the site of a precipitate in a randomly chosen section, and shows intense emission lines at 2241, 9968 and 11847 eV, corresponding to the M_α, L_α and L_β lines of mercury. The osmium M_α emission line at 1890 eV, however, is rather small relative to the mercury line. This result goes to prove that the precipitates consist predominantly of a mercuric compound, with potentially only traces of osmium in it.

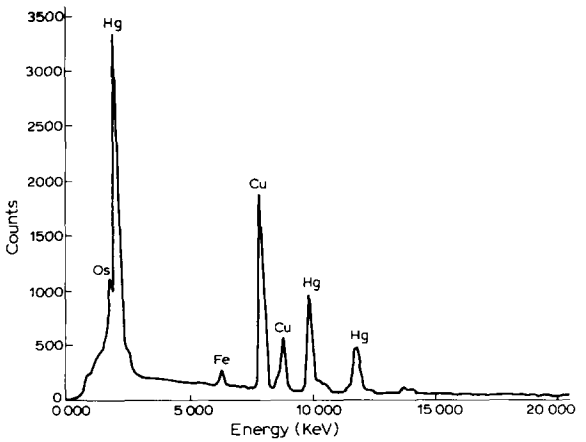

Fig. 1 Energy-dispersive X-ray spectrum of an intercellular mercuric sulphide precipitate inside a mercuric chloride- and ammonium sulphide-treated skin section LT200 sec Sample ID skin/$HgCl_2$/4212-b Peak listing

	Energy	Area	El and line	
1	0.266	237	unidentified	
2	1.890	549	Os	MA
3	2 241	9429	Hg	MA
4	6 377	471	Fe	KA
5	8 028	6433	Cu	KA
6	8.886	1596	Cu	KB or Os LA
7	9 968	3212	Hg	LA
8	11 847	1361	Hg	LB

The washing experiments Fig. 2 show that upon washing *before* in situ precipitation, most of the mercury has disappeared, with the exception of some intracellular material. However, washing *after* the precipitation did not have any significant effect on the distribution of mercury in stratum corneum and epidermis as compared to an unwashed control.

Upon overexposing the specimens to the electron beam and after sublimating the mercuric sulphide, all previously opaque sites (precipitates) had now become completely transparent, while the immediately surrounding tissue had retained its electron density (compare normally exposed and overexposed sections in Fig. 3A, B). This result shows that the precipitates were all embedded *inside* the section, and virtually excludes any delocalisation of precipitates due to the cutting procedure.

PBS-treated controls

The 1/4 h micrograph (Fig. 3C) clearly shows that initially the intercellular route predominates: the compound first enters the skin along interdigitations between apical corneocytes and it seems to be impeded in its diffusion in regions further away from these interdigitations.

After 1 h (Fig. 4A) apical corneocytes have taken up mercury; however, lower down the marker is more abundant in intercellular space and/or bound to corneocyte membranes.

After 10 h (Fig. 4B) the bimodal distribution of mercury in the stratum corneum becomes more pronounced: appreciable accumulation of homogeneously distributed mercury in apical corneocytes occurs; directly underneath there is a zone where the mercury is only present patchwise in some cells and further down in the stratum corneum the mercury is abundant between the cells and along the cell membranes.

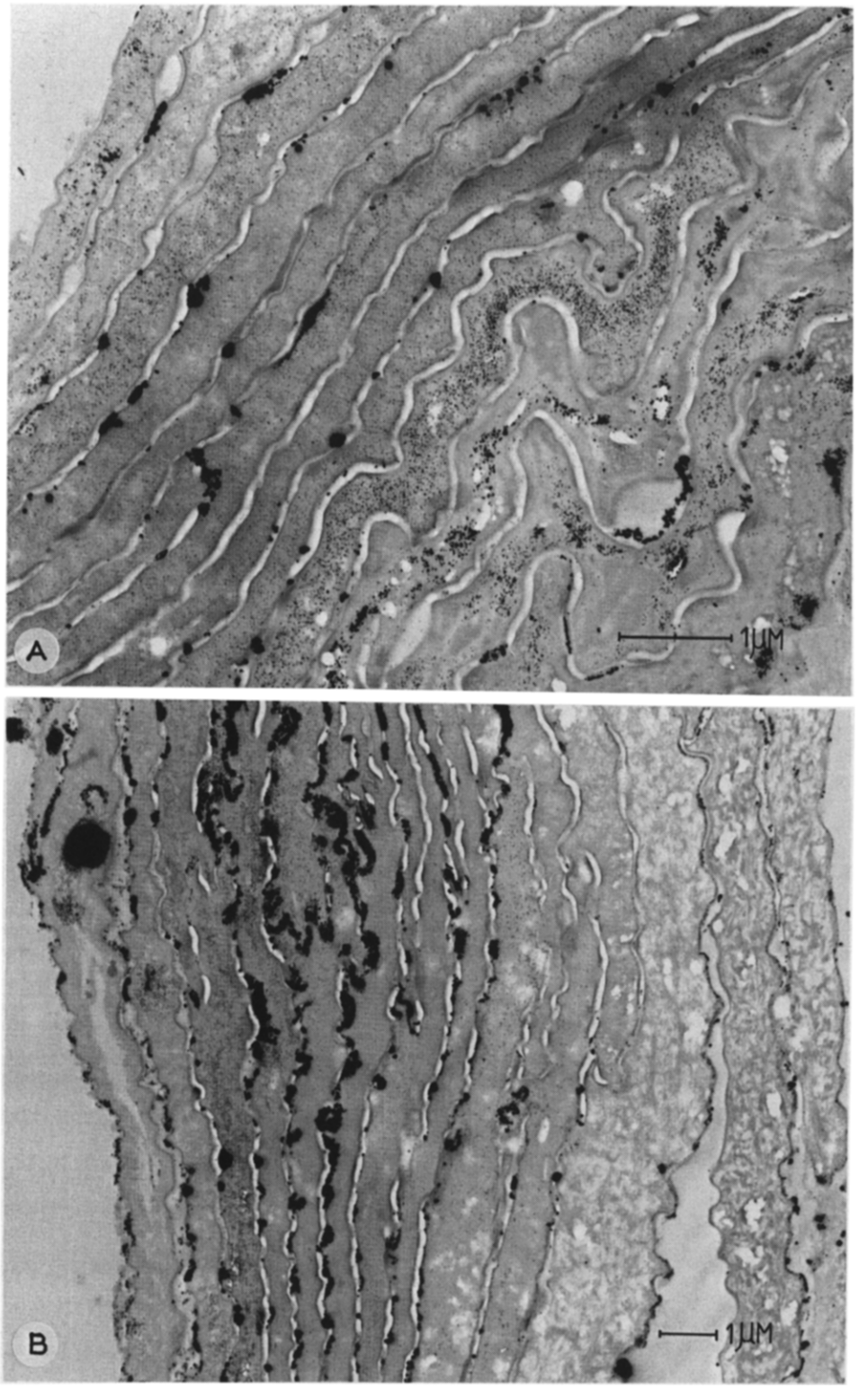

Fig. 2. Distribution of mercuric sulphide in the stratum corneum after diffusion of mercuric chloride from a 5% donor solution followed by (A) a 20 h wash in PBS prior to sulphide precipitation and (B) direct sulphide precipitation

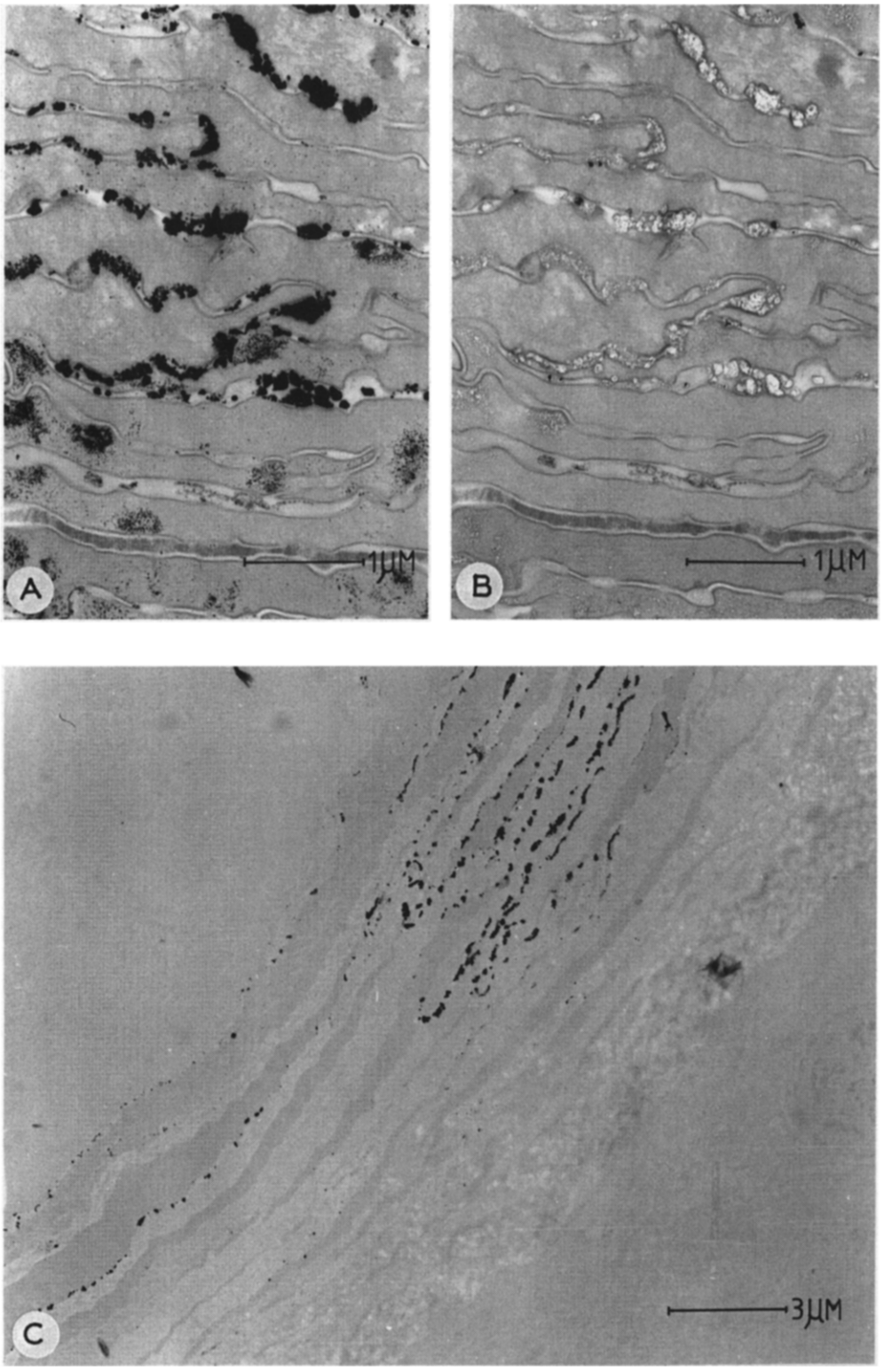

Fig. 3 Distribution of mercury in the stratum corneum. A: as observed in routine electron microscopic examination B the same section after overexposure to the electron beam, resulting in the sublimation of the mercuric sulphide precipitates The translucent zones observed match the opaque patches in the section containing HgS, thus confirming the presence of precipitates *inside* the section C: 1/4 h diffusion of mercuric chloride, showing the intercellular route of penetration (right upper side), where interdigitations are absent, there is poor penetration through the stratum corneum (left lower side).

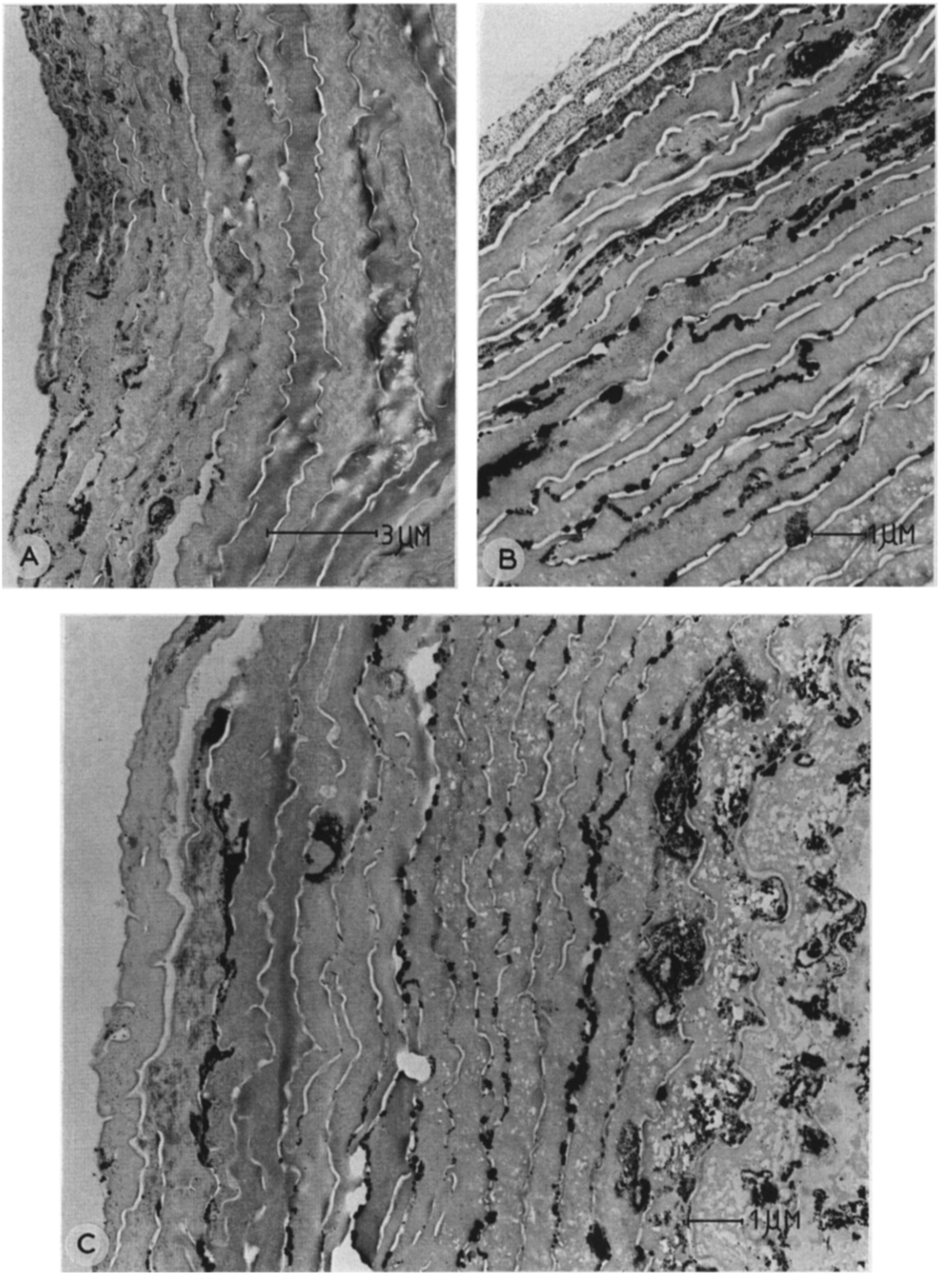

Fig. 4. A. 1 h diffusion results in mercury uptake in apical corneocytes. B: bimodal distribution of mercury after 10 h diffusion apically, most of the mercury is present in the corneocytes, medially and proximally the mercury predominates between the cells. C 10 h reverse diffusion yielding intracellular uptake in proximal and apical corneocytes and intercellular predominance of mercury between medial cells

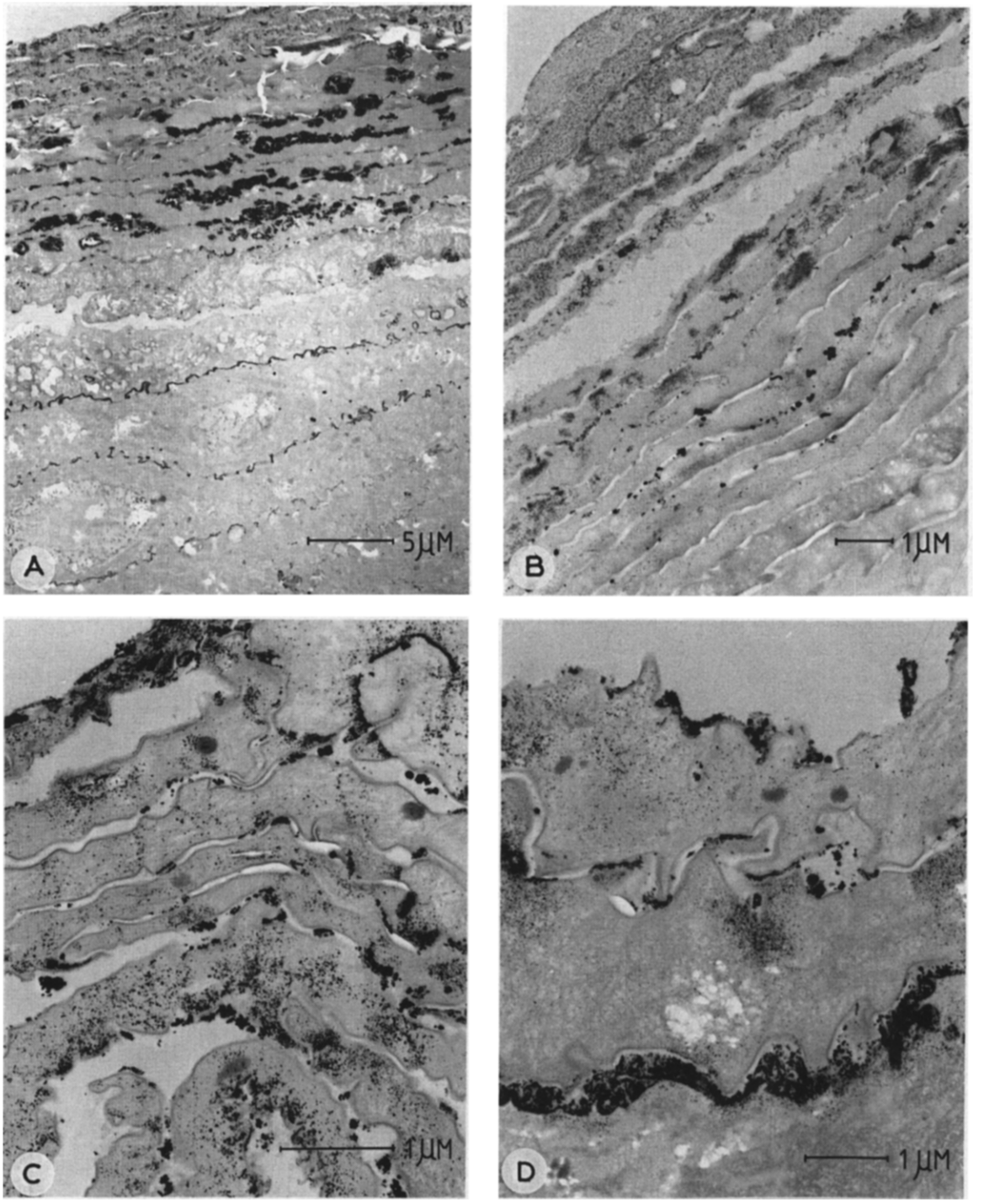

Fig. 5 A result after DMSO pretreatment, showing increased mercury penetration, without affecting the bimodal distribution observed in unpretreated skin. B result after PG treatment. C and D: results after hexyl azone pretreatment, showing enhanced penetration with intracellular mercury uptake apically (C) and intercellular penetration proximally (D).

Ten hours diffusion in the reverse direction (Fig. 4C) shows an almost "reverse" image: predominant uptake of mercury by granulocytes and proximal corneocytes, further "upwards" an intermediate zone showing intercellular abundance and finally an apical zone with some intracellular uptake.

Immersion for 1 h interestingly shows a similar distribution of mercury, namely intracellular uptake in apical corneocytes, proximal corneocytes and granulocytes, and intercellular presence inbetween. Further downwards in the spinous layer, mercury has accumulated chiefly along cell membranes and (to a lesser extent) nuclear envelopes. In fact, the characteristic undulations of the spinous cell membranes are beautifully visualised due to the mercury "staining".

Effect of DMSO

After a DMSO treatment there is (after 1 h diffusion, Fig. 5A) a significant increase in the progression of the diffusion front with respect to the PBS-treated control; in fact, the mercury has already reached the stratum spinosum and there seems to be an increase in both the intracellular mercury content in apical corneocytes, and the intercellular mercury concentration between medial and proximal corneocytes. The overall pattern very much resembles the controls obtained after 10 h diffusion (compare with Fig. 4B).

Effect of propylene glycol

The propylene glycol case does not differ significantly from the control, both qualitatively and quantitatively (Fig. 5B).

Effect of propylene glycol–azone mixtures

Hexyl azone (Figs. 5C, D) has a similar effect as DMSO in the stratum corneum, in that both the intracellular accumulation of mercury in apical corneocytes and its intercellular presence between medial and proximal corneocytes is enhanced with respect to the control. However, mercury has substantially penetrated into the viable epidermis (unlike control) and has also penetrated heavily into the viable cells and is present inside the cytoplasm (unlike control, PG and DMSO-treated specimens).

Hexadecyl azone qualitatively shows a similar pattern as the control: accumulation inside apical corneocytes, predominance of mercury between medial and proximal corneocytes.

Dodecyl azone acts differently from the others (Fig. 6A): whereas in all other cases there was always incorporation of mercury into apical corneocytes, here we have an enhanced intercellular presence of mercury throughout the stratum corneum. Massive intercellular precipitates are visible both apically and proximally in the stratum corneum.

Discussion

A striking observation that holds for most cases is the bimodal distribution of mercury within the stratum corneum: intracellular accumulation in apical corneocytes, and intercellular presence lower down. With longer diffusion or immersion times there is also uptake into proximal corneocytes. Since this phenomenon occurs in various cases, we suggest that it relates to a difference in properties of the cells and/or their membranes: apical and (especially after long diffusion times) proximal corneocytes apparently take up the model compound more easily than medial ones, either because they provide more free binding sites for the mercuric ion (possibly sulphhydril groups) or because their cell membranes are more permeable to Hg^{2+}. This bimodality may well be associated with the distinction Bowser and White (1985) have made between the stratum disjunctum and the stratum compactum; in fact, on account of their lipid analyses and water vapour transport measurements they suggested that the stratum disjunctum (the apical stratum corneum) would have a reservoir function associated with material uptake in cells, while the stratum compactum (the inner stratum corneum) would have a barrier function associated with transport of material between the cells.

From our results we can almost "reconstruct" the diffusion pathway the model compound has chosen: first, intrusion through apical interdigitations, then, slow uptake into apical corneocytes; subsequently, further diffusion through intercellu-

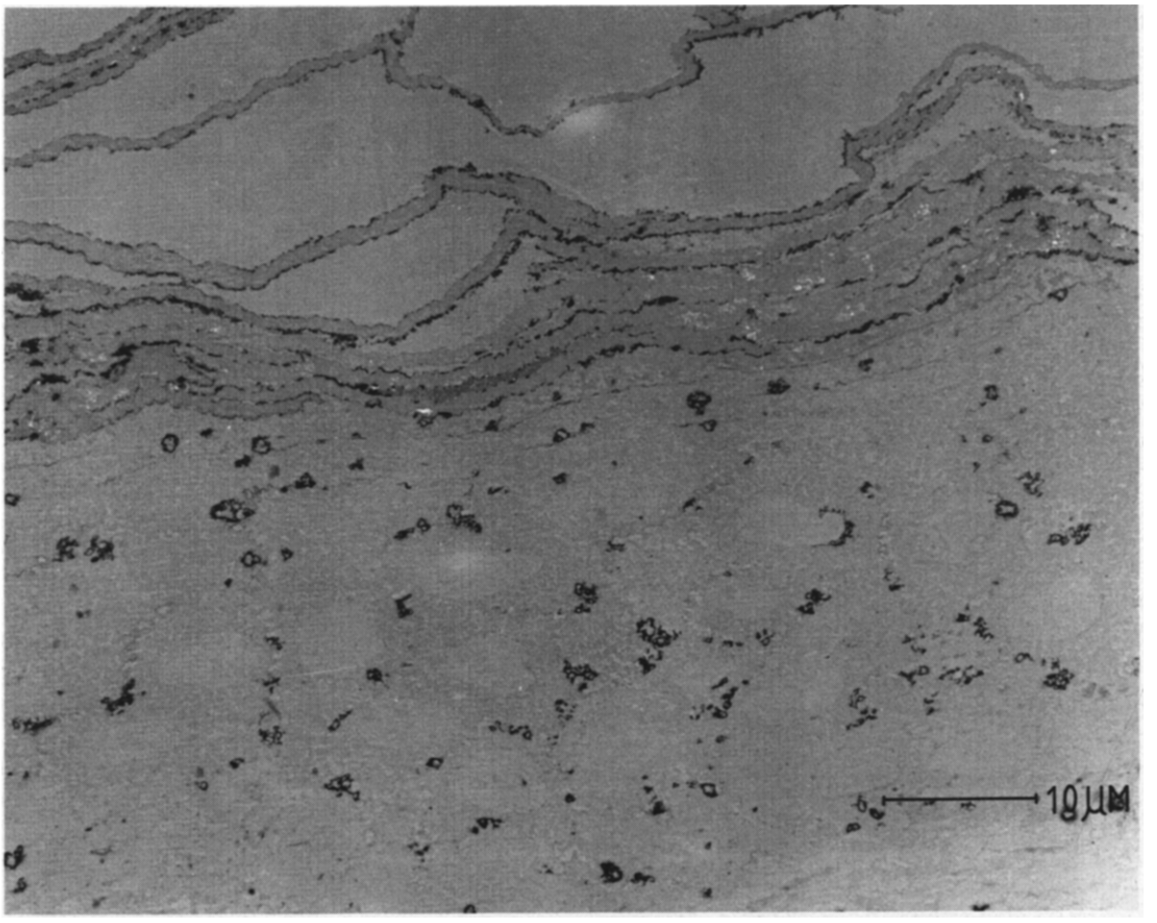

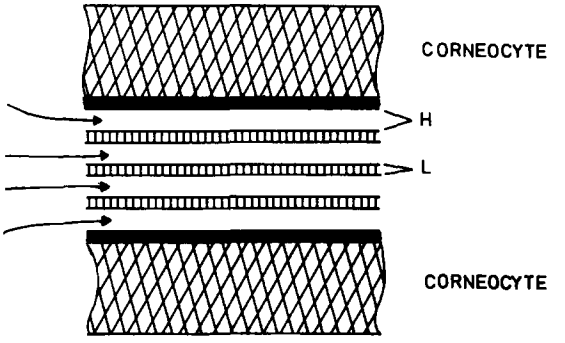

Fig. 6 A. result obtained from dodecyl azone-pretreated skin, showing enhanced intercellular transport across the entire section. B. schematic cross-section through intercellular lipid material. H = hydrophilic layers, L = lipid bilayers; arrow = possible transport route for hydrophilic substances.

lar spaces down the stratum corneum, into the viable layers; given more time, also some uptake in proximal and eventually in medial corneocytes will occur. The effect of time is especially noticeable in the "washing" experiments: upon longterm washing, thereby extending the diffusion time, most of the intercellular material has gone, showing once again the predominance of intercellular

channels as transport routes. The relatively small amounts of mercury already present in the cells are retained and possibly increased by additional uptake during 20 h washing, confirming the presence of strong binding sites inside the cells.

The fact that a hydrophilic compound permeates through lipid-rich spaces may seem peculiar at first. However, it should be borne in mind that the intercellular lipids have a lamellar structure in which both lipophilic bilayers and hydrophilic layers alternate (Williams and Elias, 1987). It may well be that Hg^{2+}, and probably any other small hydrophilic species, chooses the interlamellar hydrophilic channels (see fig. 6B). This would imply that the intercellular pathway is *bicontinuous*, consisting of a lipophilic as well as a hydrophilic route, each of which may be chosen, depending on the lipophilicity of the drug. The existence of two continuous diffusion pathways between the corneocytes (a polar and a non-polar one) has also been assumed by Barry (1987a, b, c) when addressing possible effects of penetration enhancers in the intercellular space.

In so far as mercuric chloride has penetrated into the viable epidermis, it shows a strong tendency to accumulate at the cell membranes. This tendency is possibly due to complexation of the mercuric ion with the phosphate groups of the phospholipids.

Another remarkable result from these studies is that DMSO, although enhancing the overall penetration, does not change the distribution pattern qualitatively. This contradicts the results obtained with mouse skin by Sharata and Burnette (1988), who claim that DMSO induces the keratin to swell and thereby "opens up" the corneocytes; this may well happen in our case, but then mainly in apical regions of the stratum corneum.

An explanation of the difference between the two observations obviously must lie in the origin of the skin: mouse skin is known to be much more permeable than human skin, and its lipids have a much higher fluidity; because of that, the effects of DMSO on the structure of the skin may also differ. Interestingly, our results also differ from those of Sharata and Burnette (1988) in that we do not observe "a transitional cell layer" in the stratum corneum, below which no tracer was detected. This is probably also due to the factors mentioned above.

Another interesting observation is the enhanced intercellular presence of mercury after treatment with the dodecyl azone. This may be explained as follows: given the fact that both azones have a strong influence on the intercellular lipid fluidity and structure (Bouwstra et al., 1988; Boddé et al., 1988; Beastall et al., 1988), it is assumed that it has a strong affinity for the lipid bilayers and enters these bilayers with its hydrocarbon tail, while allowing (part of) its hydrophilic headgroup to stick into the hydrophilic layer. After a PG/Azone pretreatment this interlamellar hydrophilic layer most likely consists of a propylene glycol–water mixture. The increased fluidity of the lipid bilayer may also enhance the mobility of the hydrated lipid head groups, and thereby increase the diffusivity of the hydrophilic interlamellar layers. (see also Barry, 1987a, b, c). To explain the synergistic effect of PG and dodecyl azone, Cooper (1984) and Barry (1987c) i.a. proposed that: (1) PG may solubilize dodecyl azone in the aqueous intercellular regions; (2) azone may enhance the PG flux. The present data are in line with that view. Barry (1987a and c) furthermore suggests that highly concentrated PG/azone mixtures may completely disrupt the intercellular lamellar lipid structure; recent freeze-fracture work done in our laboratory on both occlusive and non-occlusive PG/azone treatment of human skin yielded results which do not suport that notion (Boddé et al., 1988).

Why dodecyl azone seems to reduce cellular uptake of the marker while hexyl azone has no effect in that respect, cannot be explained by the data presently available.

At first it may seem remarkable that a hydrophilic compound such as mercuric chloride can be enhanced in its permeation through stratum corneum by a lipid fluidiser such as dodecyl azone. However, it should be kept in mind that the intercellular lipids serve as a *barrier*, first and foremost to prevent water loss, and furthermore to keep toxic agents out. Hence it follows that the hydrophilic pathways, which according to the literature and to the data presented here may well be the intercellular interlamellar water channels,

TABLE 1

Reaction conditions and boiling points of azones

Alkyl group	Reflux time (h)	boiling point (°C/mmHg)
Hexyl	12	113–114/0.3
Dodecyl	30	158–159/2
Hexadecyl	40	(m.p. 35 °C)

are not entirely continuous but occasionally may form 'blind alleys' possibly near interdigitations where the lipid lamellae are most likely folded around the corneocyte edges (see e.g. Williams and Elias, 1987). In fact, Fig. 3c shows that the initial diffusion behaviour of the $HgCl_2$ at interdigitations is such that the marker tends to bend around the edges of *one* of the adjacent cells, rather than spread out in all directions available at that site. This observation supports the likelihood of the aforementioned 'blind alleys' near corneocyte edges.

These may well be the sites, where lipid bilayer perturbation would strongly enhance the flux of a polar compound by allowing it to 'jump' from one hydrophilic channel to another, across the lipid bilayer.

References

Barry, B.W., Mode of action of penetration enhancers in human skin. *J. Contr. Rel.*, 6 (1987a) 85–97

Barry, B.W., Penetration enhancers: mode of action in human skin. *Pharmacol. Skin*, 1 (1987b) 121–137

Barry, B.W., Transdermal drug delivery. In P. Johnson and J.G. Lloyd-Jones (Eds.), *Drug delivery Systems, Fundamentals and Techniques* (Eds), Ellis Horwood, Weinheim, 1987c, pp. 200–223.

Beastall, J.C., Hadgraft, J. and Washington, C., Mechanism of action of azone as a percutaneous penetration enhancer: lipid bilayer fluidity and transition temperature effects. *Int. J. Pharm.*, 43 (1988) 207–213.

Boddé, H.E., Holman, B.P., Brussee, J. and Spies, F., Effects of pharmaceutical preparations on skin: an ultrastructural study, using freeze fracture electron microscopy. *Proc. Int. Symp. Controlled Release Bioact. Mater.*, 15 (1988) 276–277.

Bouwstra, J.A., Pesschier, L.J.C., Brussee, J. and Boddé, H.E., Effects of C_n-alkyl derivatives of aza-cyclo-heptan-2-one and propylene glycol on the thermal behaviour of human stratum corneum. *Int. J. Pharm.*, (1989) in press

Bowser, P.A. and White, R.J., Isolation, barrier properties and lipid analysis of stratum compactum, a discrete region of the stratum corneum. *Br. J. Dermatol.*, 112 (1985) 1–14

Cooper, E.R., Increased skin permeability for lipophilic molecules. *J. Pharm. Sci.*, 73 (1984) 1153–1156

Elling, H., Penetration of mucopolysaccharides into the skin of diverse animal species. *Drug Res.*, 36 (1986) 1525–1527

Fukuyama, K., Autoradiography. In D. Skerrow and C.J. Skerrow (Eds.), *Methods in Skin Research*, Wiley, Chichester, 1985, pp. 71–89

Golden, G.M., Guzek, D.B., Harris, R.R., McKie, J.E. and Potts, R.O., Lipid thermotropic transitions in human stratum corneum. *J. Invest. Dermatol.*, 86 (1986) 255–259

Heine, H., Experimentelle histologische Untersuchungen mit der Wirkkombination Heparin–Allantoin–D-Panthenol. *Med. Welt*, 34 (20) (1983) 2–4.

Lopp, A., Shevchuk, I. and Kirso, U., Fluorescence method for the measurement of penetration and metabolism of carcinogens in mouse skin. *Cancer Biochem. Biophys.*, 8 (1986) 185–191

Malmqvist, K.G., Forslind, B., Themmer, K., Hyltén, G., Grundin, T. and Roomans, G.M., The use of PIXE in experimental studies of the physiology of human skin epidermis. *Biol. Trace Elem. Res.*, 12 (1987) 297–308

Nemanic, M.K. and Elias, P.M., In situ precipitation: a novel cytochemical technique for visualization of permeability pathways in mammalian stratum corneum. *J. Histochem. Cytochem.*, 28 (1980) 573–578

Rick, R., Dorge, A. and Thurau, K., Regulation of transepithelial N_a transport as revealed by Electron Microprobe Analysis. In Romig Jr., A.D. and Chambers, W.F. (Eds.) *Microbeam Analysis*, San Francisco, San Francisco, 1986, pp. 209–213

Sharata, H.H. and Burnette, R.R., Percutaneous absorption of electron dense ions across normal and chemically perturbed skin. *Proc. 29th Ann. Ind. Pharm. Res. Conf.*, Merrimac, WI, U.S.A., 1987

Sharata, H.H. and Burnette, R.R., Effect of dipolar aprotic permeability enhancers on the basal stratum corneum. *J. Pharm. Sci.*, 77 (1988) 27–32

Silberberg, I., Percutaneous absorption of mercury in man. I. A study by electron microscopy of the passage of topically applied mercury salts through stratum corneum of subjects not sensitive to mercury. *J. Invest. Dermatol.*, 50 (1968) 323–331

Williams, M.L. and Elias, P.M., The extracellular matrix of stratum corneum: the role of lipids in normal and pathological function. *CRC Crit. Rev. Ther. Drug Carrier Systems*, 3 (1987) 95–122.